

## Absence of biological damage from prolonged exposure to intravascular ultrasound: A swine model

Azita Soltani <sup>a,\*</sup>, Ruchi Singhal <sup>a</sup>, Jorge L. Garcia <sup>b</sup>, Narayan R. Raju <sup>c</sup>

<sup>a</sup> Pre-clinical Research Department, EKOS Corporation, 11911 North Creek Parkway South, Bothell, WA 98011, USA

<sup>b</sup> Covance Research Products, Inc., Berkeley, CA, USA

<sup>c</sup> Pathology Research Laboratory, Inc., San Francisco, CA, USA

Received 10 April 2006; received in revised form 2 August 2006; accepted 29 October 2006

Available online 27 November 2006

### Abstract

Ultrasound (US) has been used in IMS II (intravascular US) and CLOTBUST (transcranial US) clinical trials for thrombolysis. During the treatment, in addition to the targeted thrombus, other biological components, such as blood and vessel walls are subjected to long durations of US exposure. In this study we explored evidence of biological damage due to mechanical forces or thermal effects of US exposure at the frequency, intensity and duration employed for thrombolysis treatment. Biological effects were investigated by exposing swine ilio-femoral arteries bilaterally to an intravascular US generating catheter and a conventional catheter. A total of 12 animals each underwent 8 h of exposure to intravascular pulsed US with a frequency of 2.2 MHz and spatial peak time average intensity ( $I_{SPTA}$ ) of 6 W/cm<sup>2</sup> per transducer (a total of six transducers per catheter) while the ultrasonic device surface temperature was maintained at  $\leq 43$  °C. The animals were euthanized either  $24 \pm 3$  h or  $28 \pm 3$  days post treatment. A range of physiological and hematological parameters were evaluated pre-, post-, and during US exposure. The vascular diameter was determined pre- and post-US exposure using angiograms. Following euthanasia, each animal underwent a gross pathological examination, and the treated vessels and an unexposed vessel were excised for comparative histopathological evaluation. No evidence of biological damage was found at the end of 8 h exposure to intravascular US.

© 2006 Elsevier B.V. All rights reserved.

PACS: 43.50

Keywords: Intravascular ultrasound; Exposure time; Biological effects; Swine model; Histopathological evaluation

### 1. Introduction

Ultrasound (US) has been shown to enhance the thrombolytic process *in vitro* [1,2] and *in vivo* [3]. This effect has been achieved using US alone [4] or as a thrombolytic adjuvant [1,2,5–7]. Subsequently, catheter-directed ultrasonic thrombolysis has been found to augment *in vitro* [8,9] and *in vivo* [10,11] clot lysis in combination with various thrombolytics. Despite extensive investigations, the mechanism of the prothrombolytic effect of US has not been

entirely understood [12–15]. However it has been demonstrated that thrombolytic efficacy was increased with longer US exposure time [16–18]. It is therefore relevant to demonstrate that the mechanisms responsible for prothrombolytic activity, when applied over extended therapy time, do not have the potential to cause any biological damage.

Prior testing of intravascular diagnostic ultrasound to determine acute and long term safety, has been undertaken. Intravascular diagnostic ultrasound has generally been proven safe [19,20], although sometimes has been associated with (but not necessarily the direct cause of) a minor acute clinical risk of negative effects such as vessel spasm [21]. The acoustic operating parameters in these tests were similar to those used in diagnostic ultrasound, having a

\* Corresponding author. Tel.: +1 425 415 3122; fax: +1 425 415 3103.  
E-mail address: [asoltani@ekoscorp.com](mailto:asoltani@ekoscorp.com) (A. Soltani).

frequency range of 5–40 MHz, MI of  $\sim 0.1$ , and  $I_{SPTA} \sim 4 \text{ mW/cm}^2$ . The acoustic parameters for these devices are considerably different from the Lysus<sup>®</sup> Infusion System used for this study; it is therefore necessary to investigate the safety of the specific acoustic parameters generated by this device as well.

The goal of this study was to investigate the potentially harmful effects of US by searching for evidence of biological damage after prolonged exposure to US from an intravascular ultrasonic catheter in a swine model.

## 2. Materials and methods

The study protocol was approved by the Institutional Animal Care and Use Committee (IACUC) of Covance Research Products, Inc. (Berkeley, CA). This study was carried out at Covance Research Products, Inc. and was guided by Good Laboratory Practices (GLP).

### 2.1. Test and control catheter

The test catheter was a 5.2F EKOS Lysus<sup>®</sup> catheter system (EKOS Corporation, Bothell, WA, USA) with a 6.0 cm treatment zone. This catheter system consisted of a Drug Delivery Catheter (DDC) and an UltraSound Core (USC) (Fig. 1). The DDC had a pattern of holes to deliver uniform drug flow along and around the treatment zone and a central lumen to accept the USC and to deliver coolant fluid to the USC during operation. Six US transducer elements, each with dimensions  $2.0 \times 0.4 \times 0.25 \text{ mm}$ , were mounted at evenly spaced 1 cm intervals along the USC to form the treatment zone. An EKOS PT-3 control unit was used to power the catheter system. The PT-3 control unit monitored drive power and temperature of the catheter

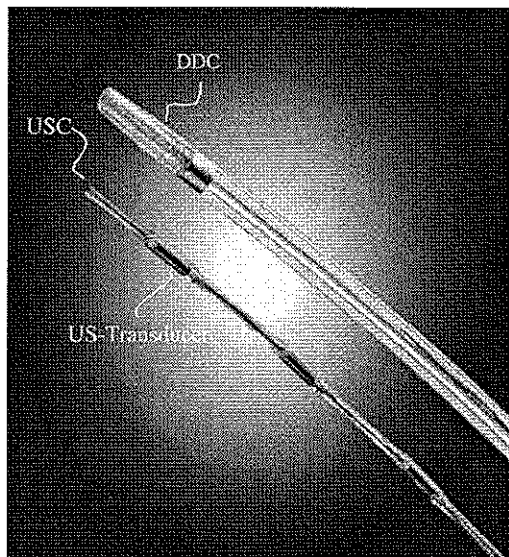


Fig. 1. EKOS Lysus<sup>®</sup> Infusion Catheter with transducer dimension of  $2.0 \times 0.4 \times 0.25 \text{ mm}$  each.

system and had safeguard circuits to prevent deviation of these parameters from preset ranges. The control catheter was a 5.0F Fountain<sup>™</sup> Infusion Catheter (Merit Medical Systems, Inc., South Jordan, Utah, USA) with a 5.0 cm treatment zone. The Merit fountain catheter was chosen as a control catheter so that we could subtract the injury due to the DDC which was similar to injury caused by this commercially available catheter. Subtracting the catheter-based injury would allow detection of injury due to prolonged intravascular ultrasound exposure.

### 2.2. Catheter temperature control

The USC and the DDC mated together in such a way that the thermocouple in one of the drug infusion lumens of the DDC was aligned with the distal end of the USC. Drug infusate passed along the transducer group and flowed over two thermocouples before being released out of tiny side holes.

The PT-3 control unit monitored the temperatures reported by the thermocouples. An algorithm used the temperature history from the thermocouples to determine the drive power applied to the transducer array. The drive power was reduced in response to temperatures approaching the preset limit ( $43 \text{ }^\circ\text{C}$ ), ensuring that the surface of the drug delivery catheter never exceeded the safe temperature for operation defined by the IEC standard for invasive ultrasonic medical devices [22].

### 2.3. Acoustic output measurement systems

**Output power measurement:** The total radiated acoustic power of each USC transducer was determined using a custom-made radiation force balance (RFB). The RFB employed a novel, thin-walled, air-backed, conical reflecting target suspended in water and connected to a gravimetric scale by a series of high-stiffness, low-weight beam structures (Fig. 2). The USC transducer was positioned within the conical compartment so that its axis of symme-

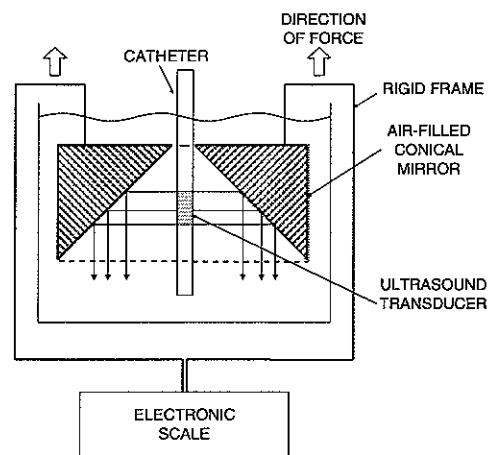


Fig. 2. Schematic of the radiation force balance.

try was aligned with that of the target. The transducer's outward-radiating acoustic field was reflected by the angled surface of the target, which produced a net upward force on the target that was measured by the scale. An acoustic absorber at the bottom of the tank prevented reflections of sound waves from interfering with the measurement. The measured force was proportional to the total radiated acoustic output power.

To verify that the full acoustic dose was delivered during treatment, the acoustic output of each USC used in this study was measured for one transducer at a time on the radiation force balance pre- and post-exposure.

**Pressure field characterization.** A hydrophone measurement of the USC's acoustic pressure field in water is shown in Fig. 3. A piezoelectric ceramic needle hydrophone (Dapco Industries, Inc., Connecticut, USA) with 0.64 mm active diameter mounted on a computer controlled 3-axis Parker positioning device and oriented toward the USC was used for this measurement. The hydrophone could be translated along three orthogonal linear axes and the USC could be rotated around its axis. The output of the hydrophone was monitored using an internal PC oscilloscope while voltage and position data were recorded using a Lab view motion control and data acquisition program. The hydrophone was calibrated using the planar scanning technique, a common method of hydrophone calibration [23] in which the beam profile is determined for a transducer of known output power. The hydrophone measure-

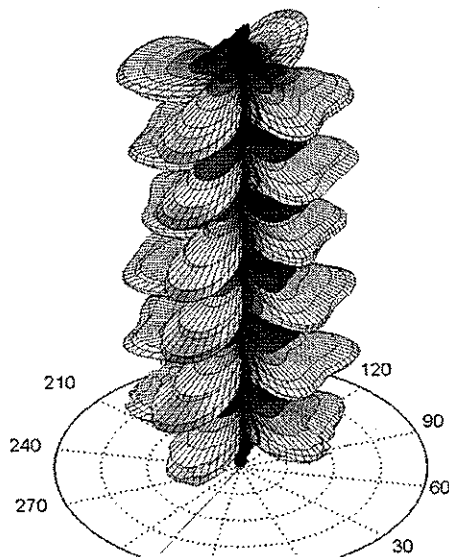


Fig. 3. A 360° acoustic pressure field map produced by six transducers mounted on USC is demonstrated. The angles are indexed relative to an arbitrary point on the catheter (at  $\theta = 0^\circ$ ). A Dapco needle hydrophone was positioned at a nominal range of 12.41 mm from the surface of the USC. The active face of the hydrophone was scanned around the USC at 120 equally spaced angular locations and repeated at 111 heights ( $dZ = 0.60$  mm) mapping out a cylindrical area that encloses all six radiating elements. Around each element two pairs of lobes were observed, corresponding to the thickness and width vibration modes for the rectangular transducers.

ment of the two-dimensional, cross-sectional beam profile for the USC transducer was related to the radiation force balance measurement of its total acoustic power to determine the hydrophone sensitivity ( $2.6 \mu\text{V}/\text{Pa}$  at 2.2 MHz). The hydrophone and USC were immersed during measurement in a tank filled with degassed water which was sufficiently large to minimize reflections.

As Fig. 3 shows, the transducers produced an acoustic field consisting of two pairs of lobes in the radial plane, corresponding to primary (thickness) and secondary (width) vibration modes for the rectangular transducer elements. For each transducer, the location of maximum pressure was directly in front of the rectangular face, corresponding to the tip of the tall narrow pair of lobes. The value of the maximum peak negative pressure was determined from the scan, and used in subsequent calculations of spatial peak acoustic field parameters for the DDC-sheathed USC (for which a reduction due to attenuation and beam spreading must be taken into account).

#### 2.4. Acoustic output values

Every transducer mounted on the USC generated millisecond-duration pulses of US of frequency of  $\sim 2.2$  MHz. After attenuation of the acoustic field through the DDC, the intensity ( $I_{\text{SPTA}}$ ) and peak negative pressure were calculated to be  $\sim 6 \text{ W}/\text{cm}^2$  and  $\sim 1.1 \text{ MPa}$ , respectively, at the interface of the Lysus<sup>®</sup> catheter system and the biological system. The resulting Mechanical Index was calculated to be  $\sim 0.7$ . The total acoustic dose intended for delivery into the vasculature over 8 h was 11.1 Wh (39.96 kJ). The acoustic power output of the test catheters was examined before, and after 8 h of exposure using the radiation force balance.

#### 2.5. Animal model

A total of 12, four month old female swine (*Suis suis*, Yorkshire crossbred) were used for this study. The animals were divided into acute and chronic groups. Acute groups were euthanized  $24 \pm 2$  h post treatment and chronic groups were euthanized  $28 \pm 3$  days post treatment. Animals were pre-medicated with 75 mg Plavix and 325 ml Aspirin by mouth once daily starting two days before the study date. Animals were pre-anesthetized with an injection of 2.5–4 mg/kg Telazol and 0.02 mg/kg Atropine followed by induced anesthesia with inhalation Isoflurane. Animals were placed in a supine position on a heating pad to maintain the body temperature during the treatment. The antimicrobial Cefazolin (20 mg/kg IV) was administered before and during surgery.

The experiments were performed using sterile procedures, except at the time of euthanasia. The jugular vein was accessed for drug and fluid delivery. The test and control catheters were both placed via an introducer in the left carotid artery into the abdominal aorta and advanced through the common iliac artery into the ilio-femoral arter-

ies. One ilio-femoral artery of each pig was exposed to the test catheter and the other was exposed to the control catheter. The placement of test and control catheters in the left or right ilio-femoral artery was alternated from one animal to the next in each cohort.

The air-filled space between the two hind limbs prevented ultrasound transmission from the test catheter to the vessel encompassing the control catheter due to the large acoustic impedance mismatch between air (0.0004 MRayl) and tissue (1.63 MRayl) which results in high reflection of ultrasound waves at the interface of these two media [24,25]. Therefore any bioeffects seen in the vessel exposed to the control catheter were not due to the ultrasound waves generated by the test catheter placed in the other hind limb. The test and control catheters were used to obtain angiograms using contrast injections. Heparinized saline (1%) was delivered continuously through the test and control catheters' drug lumen at a flow rate of 20 ml/min. Additionally, heparinized saline was delivered through the central lumen of the test catheter at 70 ml/h. Ultrasound exposure of the test catheter began simultaneously with saline delivery and continued for 8 h. To monitor the heparin anticoagulation effect, the Activated Clotting Time (ACT) assay was used to adjust heparin dose during US exposure. The ACT was maintained at a minimum of two times the baseline (pre-heparin injection value) at the discretion of the clinical veterinarian.

**Recovery:** At the completion of the 8 h US exposure the introducer insertion hole in the left carotid was repaired to allow the vessel to be patent upon recovery. At recovery each animal received 100 mg Lovenox subcutaneously, every 12 h, for 24 h to maintain the desired heparinization level. Animals surviving past the 24 h endpoint received 325 mg Aspirin and 75 mg Plavix by mouth, once a day, throughout the remainder of the study.

**Euthanasia:** Animals were anesthetized with intramuscular injections of Ketamine given at 16–20 mg/kg. After recording the physiological parameters and taking a blood sample to determine hematological values (Table 1), a lethal dose of barbituric acid was administered intrave-

nously via the ear vein. Respiratory and cardiac rates were monitored with a stethoscope until all vital signs had stopped. On dissection, the heart, liver, spleen, lungs, kidneys and the tissue surrounding the exposed vessel of the animal were photographed and examined grossly for any evidence of necrosis or damage.

The exposed arterial segments (from the iliac bifurcation to the femoral bifurcation) and a segment of unexposed (virgin) vessel taken from the brachiocephalic artery were explanted  $24 \pm 2$  h post-exposure (five animals) or  $28 \pm 3$  days post-exposure (six animals) for histopathology evaluation.

## 2.6. Biological outcome measures

Pre- and post-exposure and pre-euthanasia hematological specimens were collected. During the 8 h exposure time physiological parameters were monitored every 15 min and recorded along with the temperature of the DDC and the animal core temperature (data not shown). In addition, pre- and post-exposure angiograms were studied to determine the vascular integrity of the right and left iliac arteries.

Following euthanasia, gross examination and microscopic histopathology of serial sections of both exposed and unexposed vessel segments were performed by the pathologist in a blinded fashion. Multiple sections of the iliac and femoral arteries explants were trimmed at approximately 2 mm separation. These sections and the sections of virgin vessel taken from the left brachiocephalic artery were processed, embedded in paraffin, microtomed at approximately 4  $\mu$ m intervals and stained with hematoxylin and eosin. Several sections of each treated vessel were mounted on two slides and examined microscopically. Each damage score represents a summary of the injuries of the sections on each slide.

Injury to the vessel walls was graded using the methods established by Schwartz et al. [26]. The parameters evaluated for the damage score were as follows:

Thrombus: graded on a scale from 0 to 3.

Endothelial degeneration (ED): graded on an arbitrary scale of 0–5.

Internal elastic lamina degeneration (IELD): graded on an arbitrary scale of 0–2.

Intimal thickening (IT): graded on an arbitrary scale of 0–5.

Inflammation: graded on an arbitrary scale of 0–4.

Medial degeneration (MD): graded on an arbitrary scale of 0–3.

Adventitial degeneration (AD): graded on an arbitrary scale of 0–3.

A score of 0 indicated no damage, while the highest score indicated extensive damage, and all scores between indicated intermediate damage or changes to the tissue.

Table 1

A summary of the hematological, physiological and respiratory parameters monitored during this study

Hematological parameters	Physiological parameters
White blood cell count (WBC)	Body temperature
Red blood cell count (RBC)	Arterial blood pressure (BP)
Hemoglobin (HGB)	Heart rate (HR)
Hematocrit (HCT)	Electrocardiogram (ECG)
Mean corpuscular volume (MCV)	<i>Respiratory parameters such as:</i>
Mean corpuscular hemoglobin (MCH)	Respiratory rate (RR) & Blood
Mean corpuscular hemoglobin conc. (MCHC)	gases: (EtISO)(SaO <sub>2</sub> ), (EtCO <sub>2</sub> ),
Platelet count (PLT)	acid/base: (pH), (pCO <sub>2</sub> ), (pO <sub>2</sub> ),
Plasma protein	(HCO <sub>3</sub> ), (TCO <sub>2</sub> ), (Beb),(BEecf),
Activated clotting (ACT)	

**Statistical analysis:** To account for the fact that multiple histopathological data points were obtained from the same animal and therefore could not be treated as independent observations, the Generalized Estimating Equations (GEE) method was used to compare the EKOS and control catheter histopathology results.

### 3. Results

#### 3.1. Evaluation of animal model

For the initial four animals, the test and control catheters were both placed via the right carotid artery into the abdominal aorta and advanced through the common iliac artery into the respective ilio-femoral arteries. A diagnostic catheter, for obtaining contrast angiograms, measurement of arterial BP and blood sampling, was then inserted via the left carotid artery and positioned near the terminal aorta. One of the first four animals treated died due to cardio-respiratory arrest and the recovery of the other three was prolonged with signs of neurological

damage observed. The neurological damage was most likely to be due to prolonged anoxia to the brain from the bilateral carotid blood flow occlusion while under anesthesia. Following these observations, the procedure was simplified by placing the test and control catheter via left carotid artery, leaving the right carotid patent. Additionally, the diagnostic catheter was not used, with angiograms being obtained using contrast injections through the test and control catheters.

The six animals in the  $28 \pm 3$  days cohort showed a mild leukocytosis in their pre-euthanasia blood specimens, probably due to prolonged indoor housing.

#### 3.2. Angiography results

Angiograms were conducted pre- and post-exposure. Angiograms demonstrated no vascular spasm due to the presence of either catheters or US exposure in any of the cases. Typical examples are shown in Fig. 4a–c for the pre-exposure, post catheter placement and post-exposure of one of the animals in the 24 h cohort. A US 25 cent coin

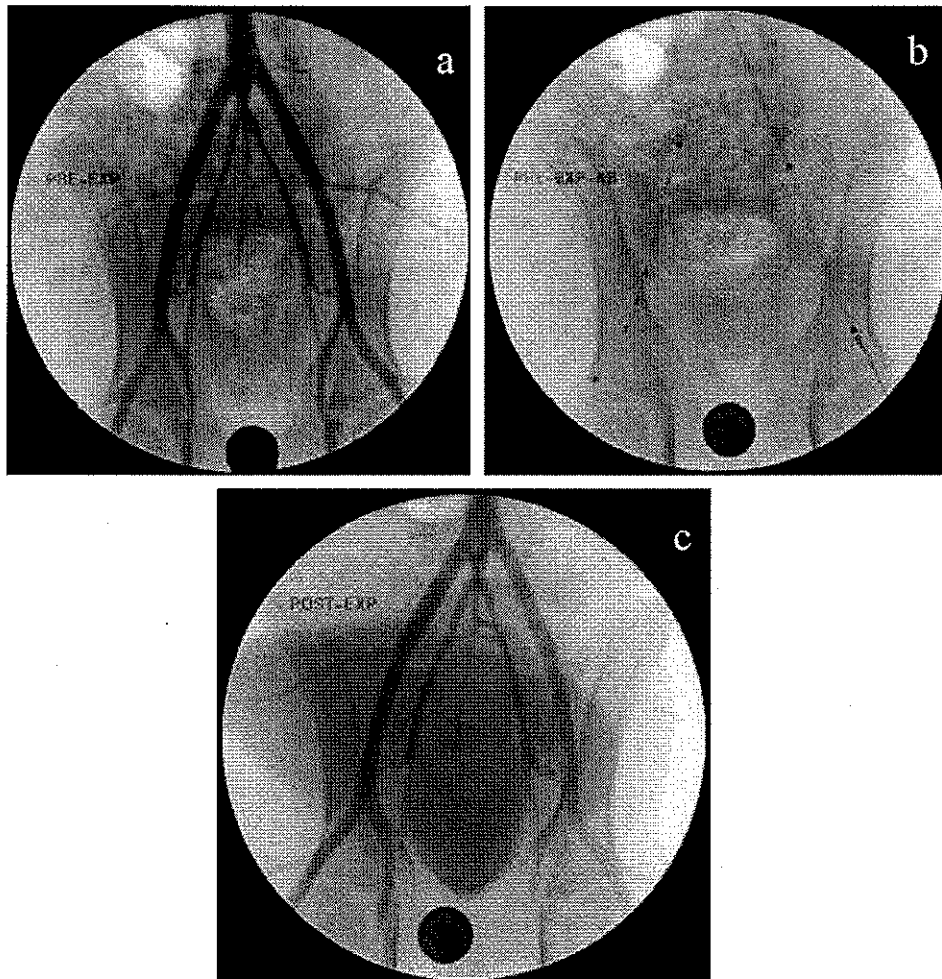


Fig. 4. Angiogram from ilio-femoral arteries of one of the animal in  $24 \pm 2$  h cohort (a) prior to catheter placement (b) post catheter placement and prior to starting US exposure (c) after completion of US exposure and removal of catheter.

(diameter of 2.3 cm) is placed in each image as a reference for dimensions.

### 3.3. Evaluation of hematological and physiological parameters

The physiological parameters and hematological values of all animals were within normal limits while under anesthesia and at pre-euthanasia.

### 3.4. Acoustic output

The average acoustic power output of the USC's transducers at the end of the 8 h US exposure time was 94.4% of the original value indicating that on average all the vessels exposed to US received in excess of 94.4% of the initial planned acoustic exposure during the 8 h (data not shown).

### 3.5. Gross pathology

For all animals tested, gross examination of the organs showed no evidence of necrosis or tissue injury that was not typically associated with the euthanasia method or dorsal recumbency. Internally, the organs of the five animals in the  $24 \pm 2$  h cohort were within the normal range of historical controls, except for one case of mild congestion of the spleen commonly associated with the method of euthanasia, and one case of moderate hypostatic congestion of the right diaphragmatic lung lobe due to lateral recumbence. The

gross pathology of the animal that died of cardio-respiratory arrest demonstrated severe diffuse pulmonary edema and a diffuse region of dark-red myocardial discoloration in the left ventricle consistent with congestion and/or hemorrhage. The six animals in the  $28 \pm 3$  day cohort demonstrated no internal gross abnormalities except for three of the pigs that demonstrated mild hypostatic congestion in the posterior dorsal aspect of diaphragmatic lobes. Such pulmonary changes are usually associated with the method of euthanasia and dorsal recumbency.

### 3.6. Histopathology

The iliac and femoral arteries explanted from the  $24 \pm 2$  h cohort (one animal excluded due to untimely death) demonstrated minimal degrees of injury localized in the vascular endothelium caused by both test and control catheters (Fig. 5a–c). Only 20% and 10% (2 and 1 out of 10 slides) of the injuries caused by test and control catheters respectively, were extended to underlying vascular walls (intima-media). In addition, minute fibrinous thrombi (Fig. 5d) and inflammation (neutrophil adhesion to the exposed vascular wall) were observed. The superficial vascular wall lesions mentioned were consistent with tissue injuries associated with intravascular device insertion and manipulation. No damage to internal elastic lamina and adventitial tissue was observed. The extent of histopathological damage for this cohort is reported in Table 2. No statistically significant difference was observed between

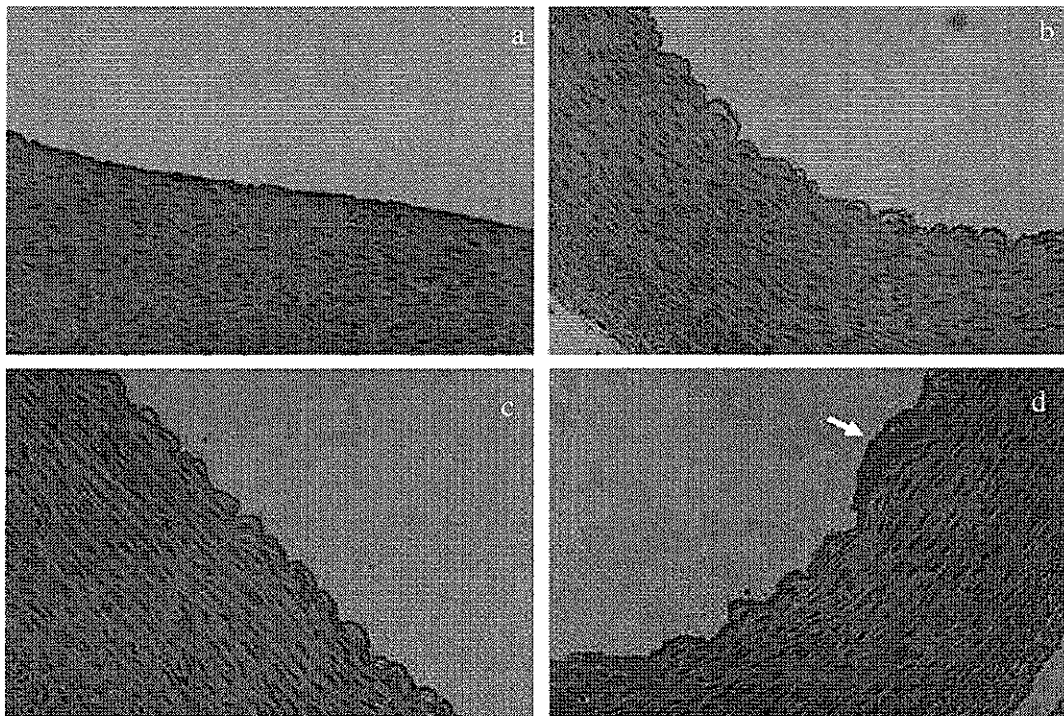


Fig. 5. Samples of the histopathological images of one of the animals in the  $24 \pm 2$  h cohort at  $30\times$  magnification (a) virgin vessel (b) vessel exposed to test catheter (c) and (d) vessels exposed to control catheter. Images b & c illustrate focal area of minimal endothelial cell loss. Image d illustrates minimal fibrinous thrombus with associated focal area of endothelial cell loss (located by arrow).

Table 2  
Histopathology score results for 24 h cohort

Score	24 h		
	0	1	2
<i>Thrombus</i>			
Test	70%	20%	10%
Control	80%	10%	10%
<i>Endothelial degeneration</i>			
Test	30%	50%	20%
Control	10%	70%	20%
<i>Intimal thickening</i>			
Test	70%	20%	10%
Control	80%	10%	10%
<i>Inflammation</i>			
Test	70%	20%	10%
Control	80%	10%	10%
<i>Medial degeneration</i>			
Test	80%	10%	10%
Control	90%	10%	0%

the extent of damage caused by the test and control catheters. The *P*-values for groups in which some damage was observed (values greater than zero) are: 0.09 for endothelial degeneration, 1 for inflammation, 0.14 for fibrinous thrombus, 0.57 for intimal thickening, 0.63 for media degeneration.

For the  $28 \pm 3$  day cohort, all vessels treated with test catheters were within normal limits and comparable with virgin vessels (Fig. 6a). 33% (4 out of 12) of control vessel segments demonstrated a minimal localized region of intimal thickening (Fig. 6b). The lesions were minute foci composed of smooth muscle cells admixed with traces of fibrin suggestive of resolving thrombi. The internal elastic lamina was intact in all cases.

All sections of the virgin vessels were within normal limits.

#### 4. Discussion and conclusion

The mechanisms that may account for profibrinolytic activity of US are suggested to be mechanical effects

[12,13], thermal effects [14] and cavitation [15]. Regarding mechanical effects, it is speculated that US could enhance thrombolysis through the process of acoustic streaming, which is the movement of drug solution in the acoustic field, or by perturbation of the thrombus exposed to the acoustic field, which would expose additional fibrin binding sites to drug molecules [12,13]. A potential adverse effect of the mechanical mechanism is that the localized shear forces resulting from acoustic streaming could cause changes in blood flow, which is known to be one of the triggers for thrombosis [27].

The thermal effect is due to absorption and conversion of US into heat within the thrombus [14]. In addition, for intravascular transducers, there is a nonacoustic source of heating due to the imperfect conversion of electrical energy to acoustic energy by the catheter transducers. However, the temperature rise due to US absorption during US-assisted thrombolysis is typically moderate, and can not be solely responsible for the observed acceleration in enzyme mediated thrombolysis [28]. Furthermore, the temperature rise due to the inefficiency of US transducers has been regulated to be  $\leq 43$  °C by IEC standards [22]. Nevertheless, even a moderately elevated temperature could affect the enzymatic activity of proteins [29] although the effect of ultrasound on plasminogen activators using the same acoustic parameters as used in this study, and its resulting moderate temperatures, has previously demonstrated no change in enzymatic activity [30]. However, protein denaturation is dependent on the temperature-time history, and a high thermal dose could adversely affect the structural stability of proteins thus contributing to cell death and tissue damage [31,32].

Cavitation is also demonstrated to have the potential to accelerate thrombolysis in addition to other mechanisms [15]. Cavitation is the activity resulting from a bubble or population of bubbles that are stimulated into action by an acoustic field [33]. However, the peak negative acoustic pressure used for this study (1.1 MPa at frequency of 2.2 MHz) is below the threshold for cavitation induction in blood [34,35]. Deng et al. reported the cavitation threshold in whole blood to be greater than 6.3 MPa at 2.5 MHz.

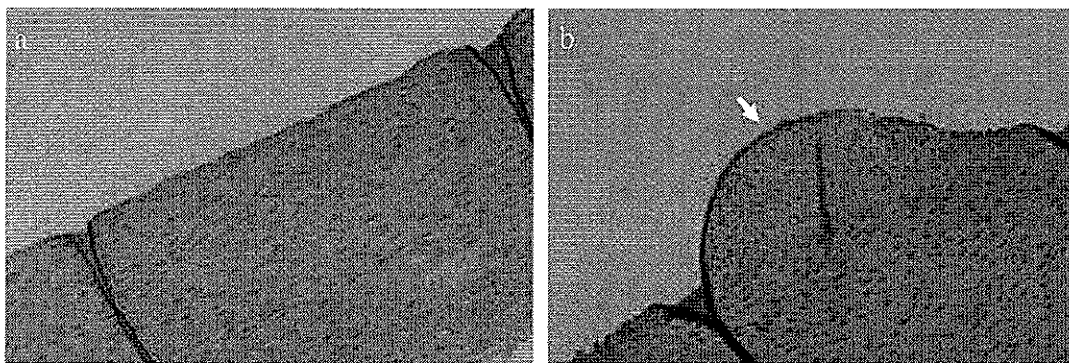


Fig. 6. Samples of the histopathological images of one of the animals in the  $28 \pm 3$  days cohort at 30 × magnification (a) vessel exposed to test catheter (b) vessel exposed to control catheter. While image a is comparable to the virgin vessel (5a) image b illustrates minimal localized region of intimal thickening (located by arrow).

The mechanisms responsible for the enhanced thrombolysis observed for the given US characteristics [2] may be one, or a combination, of the factors discussed above, but excluding cavitation. However the same mechanisms responsible for profibrinolytic activity could potentially cause adverse biological effects such as protein denaturation due to a high thermal dose or thrombus formation due to an increase in shear forces as discussed above. In the current study we looked for evidence of adverse biological damage by performing histopathological analysis of the ultrasound exposed vasculature, by using gross pathology for key organs that could be affected by denaturation of blood proteins and by investigating hematological and physiological values, in acute and chronic groups of treated animals.

No significant adverse biological effects were observed in the gross pathology of organs; histology of US exposed vessels, hematological and physiological values during 8 h of ultrasound exposure. This study demonstrates the lack of evidence for any biological damage caused by US at intensities and exposure durations sufficient to cause beneficial prothrombolytic effect.

## References

- [1] C.W. Francis, P.T. Oenunderson, E.L. Carstensen, A. Blinc, R.S. Meltzer, Enhancement of fibrinolysis in vitro by ultrasound, *J. Clin. Invest.* 90 (1992) 2063–2068.
- [2] A. Soltani, The safety of high frequency, low intensity ultrasound to enhance thrombolysis, in: *International Symposium on Therapeutic Ultrasound (ISTU) Proceedings, Boston, vol. 829, 2005, pp. 233–237.*
- [3] H. Luo, T. Nishioka, M.C. Fishbein, et al., Transcutaneous ultrasound augments lysis of arterial thrombi in vivo, *Circulation* 94 (1996) 75–77.
- [4] P. Cintas, A.P. Le Traon, V. Larrue, High rate of recanalization of middle cerebral artery occlusion during 2-MHz transcranial color-coded Doppler continuous monitoring without thrombolytic drug, *Stroke* 33 (2002) 626–628.
- [5] R. Kornowski, R.S. Meltzer, A. Chernine, Z. Vered, A. Battler, Does external ultrasound accelerate thrombolysis? Results from a rabbit model, *Circulation* 89 (1994) 339–344.
- [6] S.B. Olsson, B. Johansson, A.M. Nilsson, C.H. Olsson, A. Roijer, Enhancement of thrombolysis by ultrasound, *Ultrasound Med. Biol.* 20 (1994) 375–382.
- [7] K. Tachibana, S. Tachibana, Prototype therapeutic ultrasound emitting catheter for accelerating thrombolysis, *J. Ultrasound Med.* 16 (1997) 529–535.
- [8] R.D. Shlansky-Goldberg, D.B. Cines, C.M. Sehgal, Catheter-delivered ultrasound potentiates in vitro thrombolysis, *JVIR* 7 (1996) 313–320.
- [9] U. Rosenschein, J.J. Bernstein, E. diSegni, E. Kaplinsky, J. Bernheim, L.A. Rozenzajn, Experimental ultrasonic angioplasty: disruption of atherosclerotic plaques and thrombi in vitro and arterial recanalization in vivo, *J. Am. Coll. Cardiol.* 15 (1990) 711–717.
- [10] S. Atar, H. Luo, T. Nagai, R.A. Sahn, M.C. Fishbein, R.J. Siegel, Arterial thrombus dissolution in vivo using a transducer-tipped, high-frequency ultrasound catheter and local low-dose urokinase delivery, *J. Endovasc. Ther.* 8 (2001) 282–290.
- [11] W. Steffen, M.C. Fishbein, H. Luo, D. Lee, et al., High intensity, low frequency catheter-delivered ultrasound dissolution of occlusive coronary artery thrombi: an in vitro and in vivo study, *JACC* 24 (1994) 1571–1579.
- [12] C.G. Lauer, R. Burge, D.B. Tang, B.G. Bass, E.R. Gomez, B.M. Alving, Effect of ultrasound on tissue-type plasminogen activator-induced thrombolysis, *Circulation* 86 (1992) 1257–1264.
- [13] D. Harpaz, X. Chen, C.W. Francis, R.S. Metzler, Ultrasound accelerates urokinase-induced thrombolysis and reperfusion, *Am. Heart J.* 127 (1994) 1211–1219.
- [14] E.L. Carstensen, F.A. Duck, R.S. Meltzer, K.Q. Schwarz, B. Keller, Bioeffects in echocardiography, *Echocardiography* 9 (1992) 605–623.
- [15] E.C. Everbach, C.W. Francis, Cavitation mechanisms in ultrasound-accelerated thrombolysis at 1 MHz, *Ultrasound Med. Biol.* 26 (2000) 1153–1160.
- [16] V. Suchkova, F.N. Siddiqi, E.L. Carstensen, D. Dalecki, S. Child, C.W. Francis, Enhancement of fibrinolysis with 40-kHz ultrasound, *Circulation* 98 (1998) 1030–1035.
- [17] M. Nedelman, B.M. Eicke, E.G. Lierke, A. Heimann, O. Kempinski, H.C. Hopf, Low-frequency ultrasound induces nonenzymatic thrombolysis in vitro, *J. Ultrasound Med.* 21 (2002) 649–656.
- [18] C.W. Francis, P.T. Onundarson, E.L. Carstensen, A. Blinc, R.S. Meltzer, K. Schwarz, V.J. Marder, Enhancement of fibrinolysis in vitro by ultrasound, *J. Clin. Invest.* 90 (1992) 2063–2068.
- [19] A. Guedes, P.F. Keller, P.L. L'Allier, J. Lesperance, J. Gregoire, J.C. Tardig, Long-term safety of intravascular ultrasound in nontransplant, nonintervened, atherosclerotic coronary arteries, *J. Am. Coll. Cardiol.* 45 (2005) 559–564.
- [20] F.J. Pinto, F.G. St. Goar, S.Z. Gao, A. Chenzbaum, T.A. Fischell, E.L. Alderman, J.S. Schroeder, Immediate and one year safety of intracoronary ultrasonic imaging: evaluation with serial quantitative angiography, *Circulation* 88 (1993) 1709–1714.
- [21] D. Hausmann, R. Erbel, M.J. Alibelli-Chemarin, et al., The safety of intracoronary ultrasound, *Circulation* 91 (1995) 623–630.
- [22] IEC 60601-2-37: 2001+A1:2004(E) Part 2-37: Particular requirements for the safety of ultrasonic medical diagnostic and monitoring equipment.
- [23] IEC 61101: 1991: The absolute calibration of hydrophones using the planar scanning technique in the frequency range 0.5 MHz to 15 MHz.
- [24] L. Kinsler, A. Frey, A. Coppens, J. Sanders, *Fundamentals of Acoustics*, fourth ed., John Wiley & Sons, New York, 2000.
- [25] E. Papadakis, *Ultrasonic Instruments and Devices*, Academic Press, San Diego, CA, 1999.
- [26] R.S. Schwartz, K.C. Huber, J.G. Murphy, W.D. Edwards, A.R. Camrud, R.E. Vlietstra, Restenosis and the proportional neointimal response to coronary artery injury: results in a porcine model, *JACC* 19 (1992) 267–274.
- [27] E. Beutler, M.A. Lichtman, B.S. Coller, T.J. Kipps, *Williams Hematology*, fifth ed., McGraw-Hill, 1995, 1525.
- [28] A. Blinc, C.W. Francis, J.L. Trudnowski, E.L. Carstensen, Characterization of ultrasound-potentiated fibrinolysis in vitro, *Blood* 81 (1993) 2636–2643.
- [29] J.F. Robyt, B.J. White, *Biochemical Techniques: theory and practices*, Waveland Press, Inc., Presopect Heights, IL, 1990.
- [30] A. Soltani, C. Soliday, Effect of ultrasound on enzymatic activity of selected plasminogen activators, *Thromb. Reas.*, in Press.
- [31] N.T. Wright, J.D. Jumphy, Denaturation of collagen via heating: an irreversible rate process, *Annu. Rev. Eng.* 4 (2002) 109–128.
- [32] J.R. Lepock, K.P. Ritchie, M.C. Kolios, A.M. Rodahl, K.A. Heinz, J. Kruuv, Influence of transition rates and scan rate on kinetic simulations of differential scanning calorimetry profiles of reversible and irreversible protein denaturation, 31 (1992) 12706–12712.
- [33] T.G. Leighton, *The Acoustic bubble*, Academic Press, Inc., San Diego, CA, 1997.
- [34] C.X. Deng, Q. Xu, R.E. Apfel, C.K. Holland, In vitro measurements of inertial cavitation thresholds in human blood, *Ultrasound Med. Biol.* 22 (1996) 939–948.
- [35] J.A. Ivy, E.A. Gardner, J.B. Fowlkes, J.M. Rubin, P.L. Carson, Acoustic generation of intra-arterial contrast boluses, *Ultrasound Med. Biol.* 21 (1995) 757–767.